

# A NOVEL OFDM BLIND EQUALIZER: ANALYSIS AND IMPLEMENTATION

David E. Gonzalez Fitch, M.S. student at Bradley Department of Electrical and Computer Engineering, Virginia Tech, Blacksburg, VA 24061, USA, [davidgf@vt.edu](mailto:davidgf@vt.edu);  
 Tamal Bose, Professor and Department Head, Electrical and Computer Engineering, University of Arizona, Tucson, AZ 85721-0104, USA, [tbose@email.arizona.edu](mailto:tbose@email.arizona.edu);  
 Ashwin Amanna, Institute for Critical Technologies and Applied Science (ICTAS), Virginia Tech, Blacksburg, VA 24061, USA, [aamanna@vt.edu](mailto:aamanna@vt.edu);  
 Joseph Gaeddert, Postdoctorate at Bradley Department of Electrical and Computer Engineering, Virginia Tech, Blacksburg, VA 24061, USA, [jgaedder@vt.edu](mailto:jgaedder@vt.edu)

## ABSTRACT

Link adaptation is important to guarantee robust and reliable wireless communications without wasting valuable radio resources. This technique has become more feasible with the recent appearance of Software Defined Radios (SDRs), which allow easy reconfiguration of their parameters via software. As the environment changes over time, the transmitter needs to be able to effectively estimate its performance under different radio input parameters to be able to find a close to optimal solution. In most wireless communications, an equalizer is implemented at the receiver, which requires estimating the channel impulse response (CIR). This estimate can be fed back to the transmitter via a feedback channel, which can in turn help generate a sub-optimal transmission solution for the current situation. In this paper a new blind channel estimator specific for Orthogonal Frequency-Division Multiplexing (OFDM), based on previous work, is presented. With the use of OFDM, it can be assumed that the frequency fading at each subcarrier is approximately flat. In addition, under the assumption that the channel is quasi-stationary, the bit error rate (BER) at each subcarrier can be estimated by using the well-known BER formulas for an Additive White Gaussian Noise (AWGN) channel. However, the effect of imperfect channel estimation must also be taken into account. Finally, real over-the-air results are presented.

## 1. INTRODUCTION

The region of the electromagnetic frequency spectrum used for radio communications is becoming a scarce and ever more valuable resource. An increasing number of technologies are relying on wireless communications, leading to saturation of the radio frequency spectrum, thus it is essential to use it more efficiently. In this context, link adaptation is an innovative technique that provides robust and reliable wireless transmissions while not wasting valuable radio resources. This has become more feasible with the recent appearance of software defined radios (SDR), which allow easy reconfiguration of radio

parameters via software. As the environment changes over time, the transmitter needs to have the capability to effectively estimate performance under different radio input parameters so it can find a close to optimal solution. The main contributions of this paper were to introduce a new OFDM blind channel estimator, develop a fast and effective method of estimating the performance of these wireless communication systems for link adaptation and carry out real over-the-air tests.

The remainder of this paper is structured as follows. Section 2 presents an overview on OFDM specific blind channel estimators and equalizers. Section 3 details the developed OFDM blind channel estimator and compares its performance with the previous work it is based on. Section 4 discusses how the system can predict its own performance given that it has an estimate of the channel. Section 5 goes over the system set up to perform the over-the-air experiments. Section 6 presents performance of the channel estimator and of the predictor. Finally, section 7 summarizes and discusses areas for future research.

## 2. OVERVIEW OF OFDM SPECIFIC BLIND CHANNEL ESTIMATION

One of the main advantages of OFDM is that it allows modeling a frequency selective channel as multiple flat channels with different gains, therefore simplifying the equalization filters. A possible way of estimating the channel is by inserting pilot symbols. However, the use of pilots reduces the overall useful throughput. For this reason, blind channel estimators, which do not require the use of pilots, have been investigated. In this section, an overview of OFDM specific blind channel estimators and equalizers is presented.

Blind channel estimators can be categorized as either statistical or deterministic. The former ones require multiple received OFDM symbols to be capable of estimating the CIR, making them only suitable for quasi-static fading channels; while the latter ones can estimate the channel for each received symbol, but require very high computational complexity.

The most common way of statistical blind estimation is the subspace method, where the autocorrelation matrix of the received signal is decomposed into the signal and noise subspaces. The CIR can be estimated because the noise subspace is orthogonal to the signal subspace, which is linearly related to the CIR. An example of such a method is given in Ref. [1]. For OFDM systems without a cyclic prefix (CP) the estimation requires either time domain oversampling at the receiver or multiple receiver antennas [2], or oversampling of the frequency domain in order to reduce complexity [3].

Some of the statistical techniques exploit the cyclostationarity induced by the CP to the transmitted signal [4, 5]. Muquet *et al.* exploit the redundancy introduced by the addition of the CP by evaluating the auto-correlation matrix of the received signals [6]. Heath *et al.* introduced a subspace approach for blind channel identification using cyclic correlations at the OFDM receiver together with impulse response shortening [7].

Other types of statistical methods precode the transmitted signal and exploit its induced auto-correlation properties at the receiver to estimate the CIR. Most of these methods precode the signal without adding any redundancy, so the overall throughput of the system is not affected [8, 9, 10, 11].

Banani *et al.* developed a statistical iterative blind channel estimation technique in which a decision algorithm first makes primary symbol estimates of the data on each subcarrier based on a constrained linear minimum mean square error (MMSE) criterion [12]. These primary data estimates are then used for the MMSE channel estimation. Another iterative method is presented in [13], which is based on Independent Component Analysis, but it is for zero padding OFDM systems which transmit no information during the guard interval. A method based on the Hilbert transform for causal signals, where the amplitude and phase are related, is given in Ref. [14].

Many studies have used Kalman filters to estimate and track the channel. However, in most cases they require training symbols. One method that does not need these training symbols, and is therefore blind, is reported in [15].

Most deterministic methods for channel estimation are based on the finite alphabet property of the transmitted signal. These methods typically suffer from very high computational complexity. One example is provided in [16], where it takes into account specific properties of M-phase shift keying (M-PSK) and quadrature amplitude modulation (QAM) signals. The method of Necker and Stuber is based on the maximum likelihood principle, but it requires constant modulus modulations, otherwise it becomes too computationally complex. In addition, different modulation schemes are required for the adjacent subcarriers [17]. Wei *et al.* were able to lower the complexity by reducing the searching range for the maximum likelihood sequence [18].

Similarly, a reduced complexity minimum distance algorithm, which exploits constraints on the unwrapped phase of finite impulse response (FIR) systems, is presented in [19]. A different approach is based on the fact that the transmitted signal is confined to an allocated bandwidth, and therefore, if sampled at a sufficiently fast rate, the resulting discrete-time signal is band-limited and exhibits a smooth waveform, so the channel can be estimated via interpolation [20].

### 3. OFDM BLIND CHANNEL ESTIMATOR

In this section, a channel estimator is presented that modifies the simple linear precoding estimation introduced by Petropulu *et al.* [8]. The estimator belongs to the statistical class. It precodes the OFDM symbols and exploits the induced correlation properties at the receiver to make the estimation. The algorithm transforms the  $i^{th}$  OFDM block of  $N$  information symbols  $d_{i,k}$ , where  $k$  is the subcarrier index and its range is  $\{k = 0, \dots, N - 1\}$ , according to

$$s_{i,k} = \frac{1}{\sqrt{1+|A|^2}} (d_{i,k} + (-1)^k A q_{i,k}) \quad (1)$$

where  $A$  is a pure imaginary number with  $|A| \leq 1$  and  $q_{i,k}$  is a pseudo-randomly generated binary phase shift keying (BPSK) symbol  $\{q_{i,k} = -1, 1\}$ . Both  $A$  and  $q_{i,k}$  are predefined and assumed to be known to both the transmitter and receiver. According to Ref. [8], the precoding scheme does not modify most of the original signal's properties, such as it adds no redundancy to the data to be transmitted, it maintains the transmission power on each subcarrier, the signal is zero-mean on each subcarrier, and it adds no DC offset. However, the precoding scheme induces a known correlation that can be exploited by the receiver to estimate the channel.

The scheme presented in Ref. [8] precodes the symbols by replacing  $q_{i,k}$  with the symbol of subcarrier  $T$  ( $d_{i,T}$ ). Adding this constant to the subcarriers results in the time signal amplitude suffering from very high peaks, as can be seen in Fig. 1. These high peaks would require the quantizer to vary within a very large dynamic range, especially at high transmission powers. If the dynamic range is not wide enough, the signal will be distorted due to clipping. By using pseudo-random symbols that are different on each subcarrier, the precoded symbols derived from Eq. (1) will not suffer from this shortcoming, as shown in Fig. 2.

After the precoding step, the symbols go through the regular OFDM system model. At the receiver, after CP removal and the discrete Fourier transform (DFT) steps, the  $i^{th}$  OFDM block is:

$$y_{i,k} = H(k)s_{i,k} + v_{i,k} = \frac{1}{\sqrt{1+|A|^2}} H(k) (d_{i,k} + (-1)^k A q_{i,k}) + v_{i,k} \quad (2)$$

where  $H(k)$  is the complex gain of the  $k^{th}$  subcarrier, and  $v_{i,k}$  is the noise, modeled as a zero-mean complex Gaussian

random variable with variance  $\sigma_v^2$ . The channel is modeled

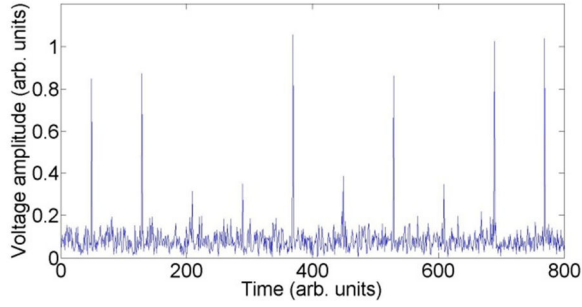


Figure 1: Time signal amplitude obtained following the precoding method of [8]

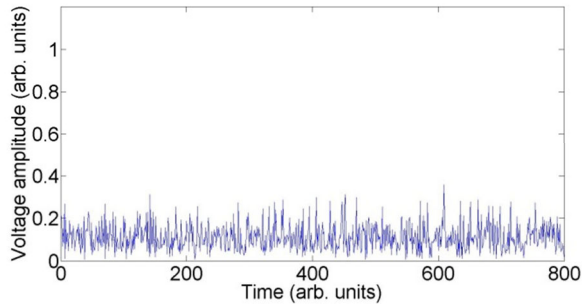


Figure 2: Time signal amplitude obtained following the precoding method described herein

as a finite impulse response (FIR) filter of length  $L$  where its tap coefficients are defined as:  $h(l), l = 0, \dots, L - 1$ ;  $H(k) = \sum_{l=0}^{L-1} h(l)e^{-j2\pi kl/N}$ . The channel does not change over the duration of at least one block, and is quasistationary between blocks.

The precoding includes a known correlation of each received subcarrier  $y_{i,k}$  with the pseudo-random symbols  $q_{i,k}$ :

$$z_k = E[y_{i,k} q_{i,k}^*] = \frac{1}{\sqrt{1+|A|^2}} \sigma_q^2 H(k) \quad (3)$$

where  $\sigma_q^2$  is the variance of  $q_{i,k}$ . Therefore, the channel can be estimated from the correlation:

$$\hat{H}(k) = \frac{\sqrt{1+|A|^2}}{\sigma_q^2 A} z_k \quad (4)$$

In Ref. [8] the channel could be estimated only up to a complex constant; to resolve this ambiguity, they propose inserting one pilot symbol. This new estimator does not suffer from this limitation. Equation 4 completely estimates the channel, making it a totally blind method.

The channel estimate in Eq. 4 can be further improved if the length of the CIR is known, by performing the inverse discrete Fourier transform (IDFT) operation on  $\hat{H}(k)$ , setting the last  $N - L$  samples to zero and then performing an  $N$ -point DFT to convert back to the frequency domain. This is known as denoising [8]:

$$\hat{H}_o(k) = \frac{1}{N} \sum_{l=0}^{L-1} \sum_{n=0}^{N-1} \hat{H}(n) e^{j2\pi ln/N} e^{-j2\pi kl/N} \quad (5)$$

To estimate the channel, the correlation can be calculated from a finite number of samples:

$$\hat{z}_k = \frac{1}{J} \sum_{i=1}^J y_{i,k} q_{i,k}^* \quad (6)$$

where  $J$  is referred to as the smoothing factor.

The performance of the proposed method is compared to that of Ref. [8]. The OFDM system has  $N = 64$  subcarriers and a cyclic prefix length  $CP = 16$ . The simulated channel is an FIR filter. The method was tested under two different channel lengths:  $L = 3$  and  $L = 6$ . Each tap was modeled as a Rayleigh random variable and then kept constant for the whole simulation. Three thousand OFDM blocks were simulated and divided into groups of  $J$  symbols each. Two different smoothing factors were tested:  $J = 100$  and  $J = 200$ . Best results were obtained for  $A = j$ , where  $j$  is the imaginary unit. To measure performance, the normalized mean square error (NMSE) is calculated:

$$NMSE = \frac{\sum_{k=0}^{N-1} |\hat{H}_o(k) - H(k)|^2}{\sum_{k=0}^{N-1} |H(k)|^2} \quad (7)$$

Figure 3 depicts a plot of the NMSE versus the signal to noise ratio (SNR) for 64-QAM, although it should be noted that the modulation scheme does not influence the NMSE. Both the present method and the one reported in Ref. [8] have approximately the same NMSE for high SNR values. However, at low SNR, the method proposed herein achieves better results. Both methods have a higher NMSE for channels with longer impulse responses. The reason for this is that the non-zero components of the channel, after the denoising step, are estimates, while the null components are exactly zero, so the longer the channel, the noisier the estimate. It was noted that the NMSE of a channel of length  $L$  is approximately  $L$  times the NMSE of a channel of length one, which is an interesting observation that will be exploited later for the estimation of the BER.

$$NMSE(L) \approx L \cdot NMSE(L = 1) \quad (8)$$

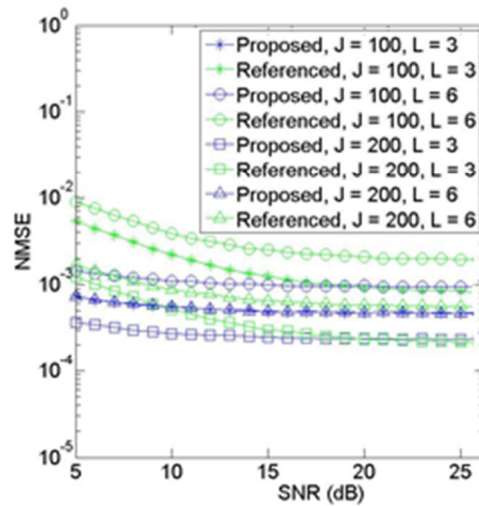


Figure 3: NMSE of the channel estimate vs. SNR

#### 4. PERFORMANCE ESTIMATION

One possible way to achieve link adaptation would be for the transmitter to estimate its performance whenever its transmission parameters are modified. A theoretical approach could be used to make this estimation. The method described here to estimate the BER improves on the one previously reported in Ref. [21].

##### 4.1 BER estimation for an uncoded transmission

To determine the overall BER of the system, the channel response at each subcarrier is assumed to be flat and quasi-static over time. In this situation, each subcarrier can be modeled as if it were to go through an AWGN channel with a different gain. Therefore, to estimate the BER per data subcarrier, which is a function of the energy per bit to noise ratio at each subcarrier  $(E_b/N_0)_{sub}$ , the system uses the well-known theoretical formulas for AWGN channels, coherent demodulation and the different modulation schemes used, which are described in Ref. [22]. The parameter  $(E_b/N_0)_{sub}$  can be calculated from the signal-to-noise-ratio per subcarrier  $(SNR_{sub})$ , the number of symbols used by the modulation scheme  $(M)$ , the system's symbol rate  $(R_S)$  and the bandwidth  $(BW)$ :

$$(E_b/N_0)_{sub} = (SNR)_{sub} + 10 \log_{10} \left( \frac{BW}{R_S \log_2(M)} \right) \quad (9)$$

The  $(SNR)_{sub}$  can be calculated from the overall system's SNR by using the estimated channel in the frequency domain at each data subcarrier. First, the channel needs to be normalized so the mean power of the channel estimate over all the data subcarriers equals one:

$$\hat{H}_{o_{norm}}(k) = \frac{\hat{H}_o(k)}{\sqrt{\frac{1}{N_{data}} \sum_{k=0}^{N-1} |\hat{H}_o(k)|^2}} \quad (10)$$

Therefore, the  $(SNR)_{sub}$  can be calculated as:

$$(SNR)_{sub} = SNR \cdot |\hat{H}_{o_{norm}}|^2 \quad (11)$$

##### 4.2. BER estimation for a coded transmission

Reference [23] describes how to calculate the word error probability  $(P_{E,C})$  for a  $t$ -error correcting code  $(n, k)$  from the digit error probability of the uncoded case  $(P_{e,U})$ . For this system, where the symbol rate remains constant, the digit error probability of the coded  $(P_{e,C})$  data equals the digit error probability of the uncoded data, so  $P_{e,U} = P_{e,C}$ .

If the data is encoded with a  $t$ -error correcting code  $(n, k)$ , the coding scheme can correct a received word that has  $t$  errors or less. Therefore, only words with more than  $t$  errors in  $n$  bits will be received incorrectly.

$$P_{E,C} = \sum_{j=t+1}^n \binom{n}{j} (P_{e,C})^j (1 - P_{e,C})^{n-j} \quad (12)$$

For block error correcting codes that use a small  $n$ , such as Hamming (7, 4), and if  $P_{e,C} \ll 1$ , the most likely event for a word received incorrectly is the occurrence of  $t + 1$  errors.

$$P_{E,C} \approx \binom{n}{t+1} (P_{e,C})^{t+1} \quad (13)$$

The previous approximation is valid because the system uses an interleaver after the forward error correction (FEC) encoding, so on the receiver side, even if burst errors occur, the deinterleaving process will spread them out.

If the received word is in error, then the decoded word of length  $k$  will also contain errors. To calculate the probability of error of the decoded data  $P_{e,D}$ , the law of total probability can be used:

$$P_{e,D} = P(e_D) = \sum_{j=0}^n P(e_D | e_C = j) \cdot P(e_C = j) \quad (14)$$

Making the same assumptions that were described previously in this subsection, Eq. (14) can be approximated to:

$$P_{e,D} \approx P(e_D | e_C = 2) \cdot P(e_C = 2) \quad (15)$$

The system was tested for data encoded with the Hamming (7, 4) scheme. In order to determine the probability of error of the decoded data if the coded word contains two errors  $P(e_D | e_C = 2)$  a simulation was run to calculate it deterministically. This simulation generated  $10^7$  uncoded words of length 4 bits and encoded them using the Hamming (7, 4) scheme. Two different random locations were generated within each coded word and its bits were flipped, so that each word always contained exactly two errors. Finally, the words were decoded and compared to the original uncoded words. It was found that the average amount of bit errors was 2.285. Therefore, the probability of error of the decoded data if the coded word contains exactly two errors can be estimated to be  $P(e_D | e_C = 2) = 2.285/4$ . Finally, the BER per data subcarrier after it was decoded  $(P_{e,D,sub})$  needs to be calculated. This is done by using the BER per data subcarrier for uncoded data  $(P_{e,U,sub})$ , which is a function of  $E_b/N_0$  and can be found in [22]. For the case where the data was encoded with the FEC scheme Hamming (7, 4):

$$P_{e,D,sub} = \frac{2.285}{4} \binom{7}{2} (P_{e,U,sub}(E_b/N_0))^2 \quad (16)$$

##### 4.3. BER estimation with imperfect channel estimate

The previously described steps to estimate performance assume that the system has perfect knowledge of the channel. In reality, the system has only an estimate, and the imperfect estimation degrades the performance. The work in [24] describes this degradation and makes it possible to quantify the signal-to-interference ratio (SIR) that it produces. Assuming the error in the channel estimation follows a Gaussian distribution, the SNR is adjusted by:

$$SIR = \frac{SNR}{1 + MSE \cdot SNR} \quad (17)$$

where MSE is the mean square error of the channel estimate, which is defined as:

$$MSE = \left\| \frac{H(k) - \hat{H}_o(k)}{H(k)} \right\|^2 \quad (18)$$

Accordingly, the BER formulas can be written as a function of SIR instead of SNR.

## 5. SYSTEM SETUP

The system is designed as a single link between two nodes, the transmitter and the receiver, and is fully described in Ref. [21]. Each node consists of a Universal Software Peripheral Device 1 (USRP1) connected to a laptop. The USRP1 is used as a flexible and affordable SDR platform often used in academic research [25]. There are several generations of USRP devices, each with a different bus speed for user data processing. For the present system, the USRP1 generation was chosen. On top of the USRP board itself, a daughter card must be used to specifically define the RF parameters that it supports. In this case, the transmitter used the RFX900 daughter card and the receiver used the WBX daughter card. Both radios used the VERT900 antenna.

*Liquid-USRP* is used as a high level interface to communicate with the USRP1s, in conjunction with *liquid-DSP*. The latter has already implemented the basic blocks for a wireless communication, and introduces a framing structure that puts them all together to send and receive data. The full tutorial on *liquid* can be found in [26, 27]. *Liquid* adds a preamble to the beginning of each packet, which allows the system to make an initial estimate of the carrier phase/frequency and timing offsets, as well as estimate the channel to equalize the data symbols. *Liquid* allows implementing an OFDM system. To do so, it defines three different types of subcarriers:

- *Null subcarriers*: This option disables the subcarrier. Its main purpose is to create guard bands on both ends of the allocated signal bandwidth to prevent aliasing during up-conversion/interpolation and to avoid interfering with adjacent bands.
- *Pilot subcarriers*: These are used for tracking slowly-varying channel effects such as carrier frequency/phase offsets and timing frequency offset that are due to a residual error from the initial estimation made by the preamble.
- *Data subcarriers*: These are used for carrying the payload, modulated with the desired scheme.

Upon the detection of a packet, the unmodified system would follow the general procedure described below:

1. Initial estimation of carrier frequency/phase and timing offsets using the preamble, and then compensation for these effects.
2. Estimation of the channel using the preamble.
3. Use of the pilots in the payload and the channel estimate to refine the estimation of the carrier

frequency/phase and timing offsets and compensate for them.

4. Equalization of each OFDM symbol in the payload

However, this process flow can no longer be followed when implementing the proposed blind channel estimator. The system first requires an estimate of the channel to be able to refine and compensate for the carrier frequency/phase and timing offsets, but the blind equalizer first needs to receive  $J$  symbols with no offsets to estimate the channel. To overcome this problem, the channel estimator implemented by *liquid* is used to equalize only the phase of the pilot subcarriers to next estimate the offsets. The data subcarriers are then compensated for the offsets, and, finally, the blind channel estimator can be used to equalize the data subcarriers. For a real system, this procedure would be totally impractical. However, one of the goals of the present work is to measure the performance of the blind channel estimator with real over-the-air results assuming that the other channel impairments have already been compensated for.

The system uses 64 subcarriers, of which 44 are data subcarriers, 6 are pilot subcarriers and 14 are null subcarriers. It should be noted that the subcarrier allocation is independent of both the frequency and bandwidth of the signal. The nulled subcarriers are located at each end of the allocated bandwidth to prevent aliasing during up-conversion/interpolation. The subcarrier located in the center of the signal bandwidth is also nulled to avoid interference from the leakage of the local oscillator. Six different types of modulation schemes were used: BPSK, QPSK, 8-PSK, 16-QAM, 32-SQAM and 64-QAM. In addition, the results were obtained for data that were not encoded with any FEC scheme and for data that were encoded with the Hamming (7, 4) scheme. The equalizer was tested for a smoothing factor  $J = 100$ .

The denoising step that was described in Section 3 to refine the channel estimate can no longer be performed when adding the null subcarriers. The reason for this is that the system does not have an estimate of the channel gain at the location of the null subcarriers, so it can no longer perform the IDFT operation on the frequency domain channel estimate. Accordingly, for the over-the-air experiments, to denoise the channel estimate, the corresponding amplitude at each subcarrier was fitted to a polynomial curve of order four.

The distance between the transmitter and receiver radios was about 3 ft. This short distance was chosen in an attempt to mitigate the clipping distortion as much as possible. Since this distortion was found to occur predominantly at the transmitter, the radios needed to be near each other to avoid having the transmitter use higher gains while still ensuring good SNR values.

For the proposed equalizer to work correctly, the pseudo-randomly generated symbols  $q_{i,k}$  used to precode

the information-bearing symbols needed to be known by both the transmitter and the receiver. To do so, the sequence of symbols  $q_{i,k}$  was always the same and would restart from the beginning for each packet. The used sequence had a length of 17 symbols:  $\{1, 1, -1, 1, 1 - 1, 1, 1, -1, 1, -1, -1, -1, 1, -1, 1, -1\}$ .

### 5.1. Issues to be considered for over-the-air transmissions

Many variables that are hard to model and thus are not considered in simulations can be responsible for undesirable effects in over-the-air transmissions, degrading performance. For instance, the hardware used by the USRP1s has some deficiencies and limitations. The oscillators at the transmitter and receiver, when set at the same frequency, do not operate at exactly that frequency, but will each have a different small offset. In theory, this should not be an issue because the receiver can estimate the frequency offset and compensate for it. However, the error in the estimation of the frequency offset increases with increasing frequency offset. Therefore, to reduce this error, the center frequency of the receiver was manually adjusted to achieve a frequency offset as close as possible to zero. The center frequency of the transmitter was set to 910.0000 MHz, and the center frequency of the receiver was set to 910.0037 MHz.

Another problem can occur if the transmitter laptop feeds data to the USRP1 at too slow a rate; this will cause the radio to emit "junk" data, where it will transmit anything it has in its outdated buffer, generating what are known as underruns. Alternatively, if the USRP1 on the receiver side feeds data to the laptop at too fast a rate to process, then some of the data gets dropped and lost, producing what are known as overruns. Both situations will cause a higher BER than what will be predicted by the system. To make sure these situations do not occur, the bandwidth needs to be reduced, because it is well known that, for a constant spectral efficiency, a narrower bandwidth means a slower throughput, so the USRP1s will need fewer samples, lowering the burden on the laptops. On the other hand, OFDM systems with narrower bandwidths are more sensitive to a frequency offset, so a compromise needs to be found. It was determined experimentally that an adequate bandwidth for the system was 100 kHz.

For an OFDM system with a bandwidth  $BW = 100$  kHz and with  $N = 64$  subcarriers, the bandwidth per subcarrier would be  $BW_{sub} = BW/N = 1.5625$  kHz. Therefore, since electromagnetic waves propagate at the speed of light  $c = 3 \cdot 10^8$  m/s, for the channel to exhibit multipath characteristics, the separation between multipath components should be at least  $BW_{sub} = 192$  km. At such a large distance, the multipath components will be so

attenuated that they will not have any discernible effect. This means that for the chosen bandwidth, the channel is effectively flat. However, the USRP1 hardware will deform this flat channel response. More specifically, the part of the digital circuitry that has the main effect on this distortion is the cascaded integrator-comb (CIC) filter in the field-programmable gate array (FPGA), causing the channel response in the frequency domain to "droop" on both ends of the allocated bandwidth.

It is well known that OFDM signals have a high peak-to-average power ratio due to the overlap of multiple sinusoids [28]. The transmit power amplifier needs to be linear across the whole signal range, otherwise it will clip the peaks of the signal, causing distortion. This clipping problem is especially apparent at higher transmission powers where the range of the amplifier needs to be wider. Therefore, the transmitter USRP1 will clip the signal at higher powers, causing the BER to increase instead of decrease. Also, OFDM symbols modulated at higher modulation orders have a higher peak-to-average ratio, so they suffer from more distortion caused by clipping for the same transmission power. For results that will be shown later on in this paper, this clipping region will be omitted.

## 6. RESULTS

This section describes the achieved performance of the system in terms of BER using the proposed equalizer, and compares it to the predicted performance of the system. Figure 4 shows an example of the channel estimate. It compares the initial channel estimate, in blue, with the smoothed estimate, in green. The frequencies of the null and pilot subcarriers are denoted with red circles. At these locations, the channel is not estimated because the received signal does not have the expected correlation characteristics that would be required.

For the BER prediction, the SNR needs to be adjusted as described in Eq. (17). From the simulations presented in Section 3, it is known that the NMSE, and therefore the MSE, is constant, and independent of the channel. Therefore, the MSE defined in Eq. (18) is adjusted manually. It was noted that the effective channel length was  $L = 3$ . Thus, to adjust the MSE, the  $MSE(L = 1)$  was found manually, and the total MSE for any value of  $L$  was then calculated following a procedure similar to that used to determine NMSE (see Eq. (8)). The system was tested for different values of  $J$ , and it was found that, contrary to the simulation results, the system performance was virtually the same for values of  $J = \{100, 200, 500\}$ . Therefore, the results presented in this section are only for  $J = 100$ . The MSE was adjusted as described previously, and the resulting value was 0.013.



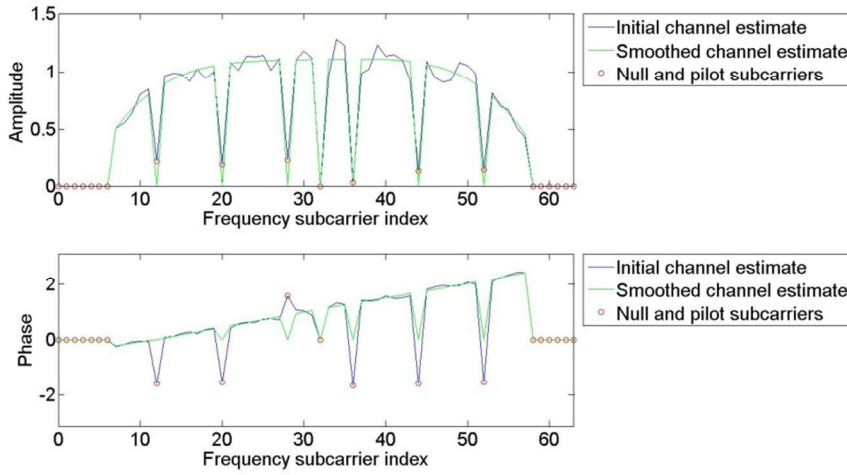


Figure 4: Example of a channel estimate

The blue curves in Figs. 5 and 7, depict the measured BER for each of the six different modulation schemes that were tested, while the green curves show the BER estimated by the system using Eq. (17) to adjust the SNR. The error floor is due to the imperfect channel estimate. The proportional error between the estimated and measured BER, in dB, is defined as:

$$\varepsilon_{BER} = 10 \log_{10} \left( \frac{BER_{estimated}}{BER_{measured}} \right) \quad (19)$$

This error is shown in Figs. 6 and 8. The error is generally within the range of -5 dB and 5 dB, and almost always within the range of -10 dB and 10 dB. This implies that the error in the estimate is smaller than the order of magnitude of BER. In general, the predictions work better for the  $M$ -PSK schemes than for the QAM schemes. This could be due to the larger peak-to-average ratio of QAM, which could cause some clipping effects to occur. Also, for the tests where the data was coded, the predictor performance is worse for higher modulation schemes because it is more likely that there are more than  $t+1$  errors, which was the assumption that was made previously to estimate the BER.

## 7. ACKNOWLEDGEMENTS

This work received support from the Federal Rail Association through Grant # 1234.

## 8. CONCLUSIONS AND FUTURE WORK

The work described herein presents a novel blind channel estimator using a statistical method that improves on the one previously introduced by Petropulu *et al.* [8]. It is a simple method that is not difficult to implement. However, it requires extra computation processing at the receiver to buffer the OFDM symbols and then to equalize them all at once when the system has a channel estimate.

In contrast with many other studies that simply run simulations, here, over-the-air tests were performed and real experimental results were obtained. The performance, measured in terms of the BER, was satisfactory and opens the way to possible improvements in the future. The equalizer was also found to work well in a real world environment.

In addition, a method has been proposed to predict how the system will perform, given that it knows the SNR and it has an imperfect estimate of the communication channel for data that is either uncoded or coded with a FEC block code, such as the Hamming (7, 4) scheme. It was found that the predictions, for BER of as low as  $10^{-6}$ , were generally within the same order of magnitude for all modulation schemes. These predictions could be used in combination with a Cognitive Engine to perform link adaptation, optimizing the transmission parameters controlled by the system.

While the proposed equalizer is blind, some other issues that are present in real world communications, such as the frequency/phase and timing offsets, require the presence of pilot subcarriers. To make the proposed system truly blind, however, methods to estimate the frequency/phase and timing offsets without the presence of pilots should be investigated. Other blind channel equalizers, based on either statistical or deterministic methods, could also be implemented and tested over-the-air to compare their performance.

The hardware used for the tests presented many limitations, especially in the case of an OFDM transmission, which is known to have a high peak-to-average ratio, thus the radios could have been distorting the signal due to clipping or other nonlinear effects. The system should be tested with better hardware, such as USRP-2 (the second generation of USRPs) or other radios, to measure if performance is improved.

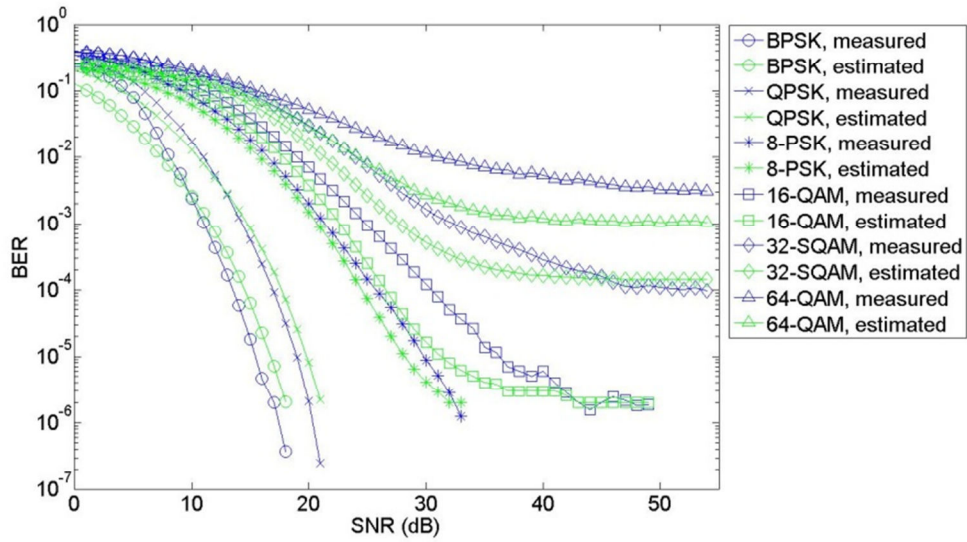


Figure 5: Measured and estimated BER for uncoded data, for the six tested modulation schemes and  $J = 100$

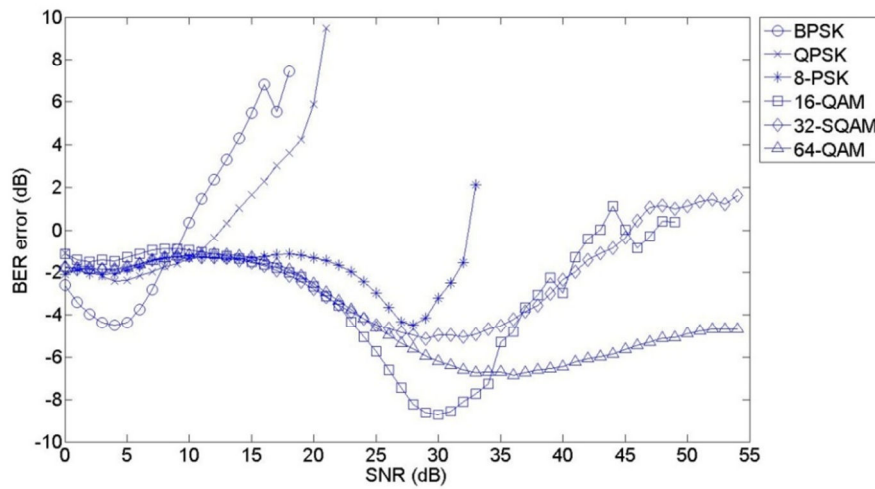


Figure 6: Error between the estimated and measured BER for uncoded data, for the six tested modulation schemes and  $J = 100$



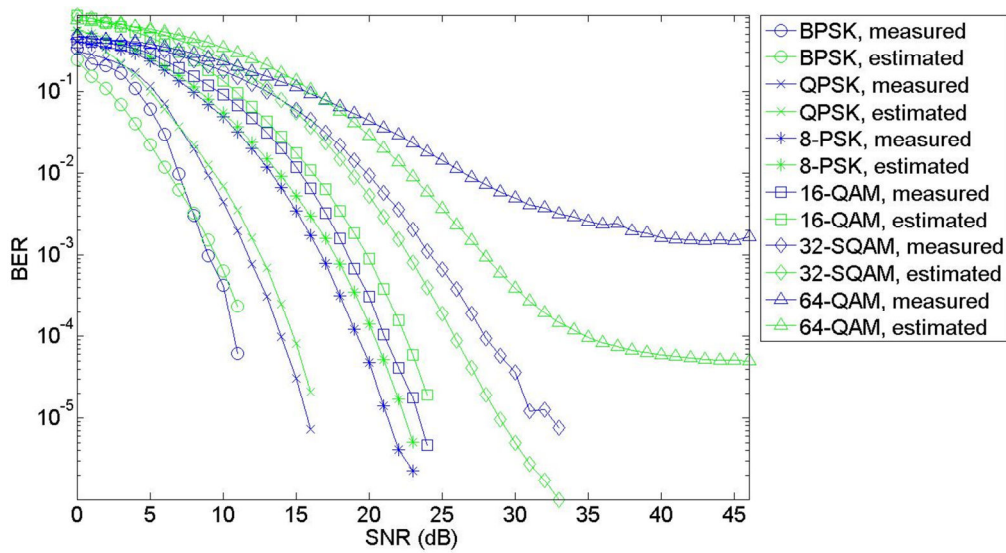


Figure 7: Measured and estimated BER for data that was encoded with Hamming (7, 4), for the six tested modulation schemes and  $J = 100$

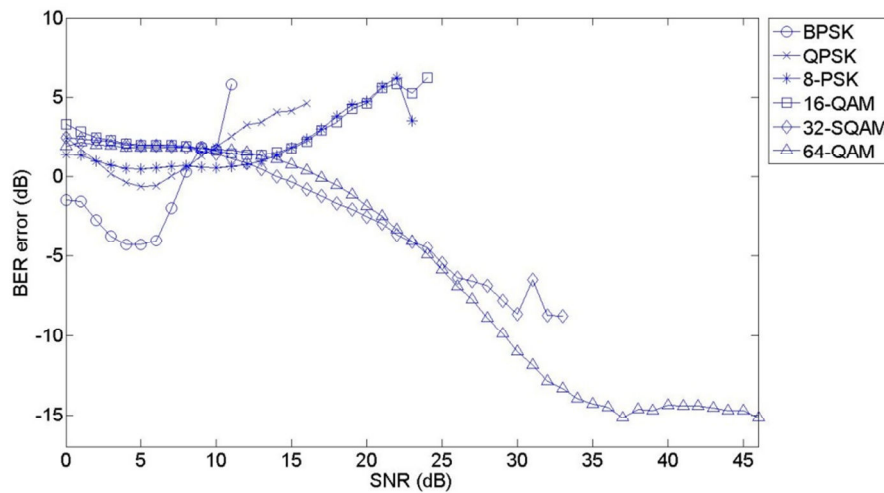


Figure 8: Error between the estimated and measured BER for data that was encoded with Hamming (7, 4), for the six tested modulation schemes and  $J = 100$

## 9. REFERENCES

- [1] B. Muquet, M. de Courville, and P. Duhamel. Subspace-based blind and semi-blind channel estimation for ofdm systems. *Signal Processing, IEEE Transactions on*, 50(7):1699–1712, jul 2002.
- [2] Chengyang Li and S. Roy. A subspace blind channel estimation method for ofdm systems without cyclic prefix. In *Vehicular Technology Conference, 2001. VTC 2001 Fall. IEEE VTS 54th*, volume 4, pages 2148–2152 vol.4, 2001.
- [3] Qinghua Shi, Y. Karasawa, and Ying Wang. Blind channel and frequency offset estimation for ofdm via frequency-domain oversampling. In *Wireless Communications Networking and Mobile Computing (WiCOM), 2010 6th International Conference on*, pages 1–5, sept. 2010.
- [4] F.O. Alayyan, K. Abed-Meraim, and A.M. Zoubir. Blind equalization in ofdm systems exploiting guard interval redundancy. In *Signals, Systems and Computers, 2005. Conference Record of the Thirty-Ninth Asilomar Conference on*, pages 697–700, 28 2005-nov. 1 2005.
- [5] F.O. Alayyan, K. Abed-Meraim, and A.M. Zoubir. Blind equalization and frequency offset estimation in ofdm systems exploiting guard interval redundancy. In *Signal Processing and Its Applications, 2005. Proceedings of the Eighth International Symposium on*, volume 1, pages 135–138, 28-31, 2005.
- [6] B. Muquet and M. de Courville. Blind and semi-blind channel identification methods using second order statistics for ofdm

- systems. In *Acoustics, Speech, and Signal Processing, 1999. Proceedings., 1999 IEEE International Conference on*, volume 5, pages 2745–2748 vol.5, 1999.
- [7] Jr. Heath, R.W. and G.B. Giannakis. Exploiting input cyclostationarity for blind channel identification in ofdm systems. *Signal Processing, IEEE Transactions on*, 47(3):848–856, mar 1999.
- [8] A. Petropulu, Ruifeng Zhang, and R. Lin. Blind ofdm channel estimation through simple linear precoding. *Wireless Communications, IEEE Transactions on*, 3(2):647–655, march 2004.
- [9] S. Ghadrdran, M. Ahmadian, S. Salari, and M. Heydarzadeh. An improved blind channel estimation algorithm for ofdm systems. In *Telecommunications (IST), 2010 5<sup>th</sup> International Symposium on*, pages 421–425, dec. 2010.
- [10] Zhou Jing, Chang Yongyu, Zhe Chen, and Dacheng Yang. Joint blind channel estimation and turbo equalization for ofdm systems. In *Vehicular Technology Conference Fall (VTC 2010-Fall), 2010 IEEE 72nd*, pages 1–5, sept. 2010.
- [11] F.J. Simois, J.J. Murillo-Fuentes, R. Boloix-Tortosa, and L. Salamanca. Near the cramer-rao bound precoding algorithms for ofdm blind channel estimation. *Vehicular Technology, IEEE Transactions on*, 61(2):651–661, feb. 2012.
- [12] S.A. Banani and R.G. Vaughan. Ofdm with iterative blind channel estimation. *Vehicular Technology, IEEE Transactions on*, 59(9):4298–4308, nov. 2010.
- [13] R. Boloix-Tortosa, F.J. Simois-Tirado, and J.J. Murillo-Fuentes. Blind adaptive channel estimation for ofdm systems. In *Signal Processing Advances in Wireless Communications, 2009. SPAWC '09. IEEE 10th Workshop on*, pages 191–195, june 2009.
- [14] Chen Wei. Fast blind channel estimation based on discrete hilbert transform in ofdm system. In *Communications and Mobile Computing (CMC), 2010 International Conference on*, volume 3, pages 21–23, april 2010.
- [15] R. Zhang and W. Chen. A mixture kalman filter approach for blind ofdm channel estimation. In *Signals, Systems and Computers, 2004. Conference Record of the Thirty-Eighth Asilomar Conference on*, volume 1, pages 350–354 Vol.1, nov. 2004.
- [16] Shengli Zhou and G.B. Giannakis. Finite-alphabet based channel estimation for ofdm and related multicarrier systems. *Communications, IEEE Transactions on*, 49(8):1402–1414, aug 2001.
- [17] M.C. Necker and G.L. Stuber. Totally blind channel estimation for ofdm on fast varying mobile radio channels. *Wireless Communications, IEEE Transactions on*, 3(5):1514–1525, sept. 2004.
- [18] Li Wei, Chen Ming, Shixin Cheng, and Haifeng Wang. A complexity reduced blind channel equalization scheme for ofdm systems. In *Personal, Indoor and Mobile Radio Communications, 2006 IEEE 17th International Symposium on*, pages 1–4, sept. 2006.
- [19] Seongwook Song and Andrew C. Singer. Blind ofdm channel estimation using fir constraints: Reduced complexity and identifiability. *Information Theory, IEEE Transactions on*, 53(3):1136–1147, march 2007.
- [20] H. Murakami. Deterministic blind channel estimation for a block transmission system using fractional sampling and interpolation. *Signal Processing, IEEE Transactions on*, 55(10):4969–4978, oct. 2007.
- [21] S.S. Das, M.I. Rahman, Yuanye Wang, F.B. Frederiksen, and R. Prasad. Hybrid strategies for link adaptation exploiting several degrees of freedom in ofdm based broadband wireless systems. In *Vehicular Technology Conference, 2007. VTC-2007 Fall. 2007 IEEE 66th*, pages 1807–1811, 30 2007-oct. 3 2007.
- [22] ThomasW. Rondeau. *Application of Artificial Intelligence to Wireless Communications*. PhD thesis, Virginia Tech, Blacksburg, VA, 2007.
- [23] Bhagwandas Pannalal Lathi. *Modern Digital and Analog Communication Systems*. Oxford University Press, 3rd ed. edition, 1998.
- [24] A. Leke and J.M. Cioffi. Impact of imperfect channel knowledge on the performance of multicarrier systems. In *Global Telecommunications Conference, 1998. GLOBECOM 1998. The Bridge to Global Integration. IEEE*, volume 2, pages 951–955 vol.2, 1998.
- [25] M. Ettus. Ettus research. <http://www.ettus.com/>, 2012.
- [26] Joseph D. Gaeddert. liquid-dsp. <https://github.com/jgaeddert/liquid-dsp>, June 2012.
- [27] Joseph D. Gaeddert. liquid-usrp. <https://github.com/jgaeddert/liquid-usrp>, June 2012.
- [28] Mahesh K Banavar Narasimhamurthy, Adarsh B and Cihan Tepedelenliolu. *OFDM Systems for Wireless Communications*. Morgan & Claypool Publishers, San Rafael, Calif. (1537 Fourth Street, San Rafael, CA 94901 USA), 2010.